International Journal on Recent and Innovation Trends in Computing and Communication
ISSN: 2321-8169 Volume: 11 Issue: 7
Article Received: *25 January 2023* ***Revised:*** *12 March 2023* ***Accepted:*** *30 June 2023*

Enhancement of Power Quality using Solar Photovoltaic System with Universal Active Filtering and Fuzzy Logic Controller Capabilities

***Mr. D Venkatabrahmanaidu[1]*, Dr.R.Thamizhselvan[2] , Dr.Ch. Chengaiah[3,]**
[1]Research Scholar, Department of Electrical Engineering, Annamalai University, Tamil Nadu, India.
e-mail: dvb.naidupeed@gmail.com (corresponding author)
[2]Associate Professor, Department of Electrical Engineering, Annamalai University, Tamil Nadu, India.
e-mail: rt10535@annamalaiuniversity.ac.in
[3]Professor, Department of Electrical and Engineering, S.V.U College of Engineering,
Sri Venkateswara University, Tirupati, India.
e-mail: chinthapudisvu@gmail.com

Abstract: This work proposes a novel technique for controlling the universal active power filter integrated with PV array system (UAPF-PV), which is based on a second-order sequence filter and a proportional resonant controller. The active component of the distorted load current is estimated using a second order sequence filter, The Fuzzy Logic Controller is used to estimate the loss component and this information is then used to provide a reference signal for a shunt active filter at the instant of zero crossing of the load voltage. With fewer mathematical calculations, the suggested method extracts the essential active component of distorted and unbalanced load currents with good accuracy. In addition to enhancing power quality, the system produces clean energy through the PV array system that is built into its DC-bus. The benefits of distributed generation and power quality improvement are combined in the UAPF-PV system. MATLAB/Simulink is used to assess the system performance under a range of disturbance scenarios, including changes in solar irradiation, load unbalancing, and PCC voltage rise and fall.

Keywords : *power quality, universal active power filter,adaptive filtering, photovoltaic system, fuzzy logic controller, maximum powerpointtracking, sequence filter*.

I. Introduction

Installing renewable energy sources, such as grid-connected wind and solar photovoltaic systems, has become more and more important [2]. This has been made possible by the advancement of dependable and effective power electronics, increased photovoltaic panel efficiency, and declining production prices. However, variations in voltage at the point of common coupling (PCC) have also increased with the growing penetration of renewable energy sources, which are sporadic energy sources. This is especially typical in distribution systems with low voltage. The widespread use of nonlinear power electronic equipment, which draw extremely distorted currents, is another significant problem with contemporary distribution networks. Depending on the amount of current and grid impedance, these distorted currents may result in voltage distortion at PCC [3].These loads can result in losses in distribution transformers and feeders. Furthermore, the sensitivity of these loads to PCC voltage dips and rises results in frequent tripping and higher maintenance expenses. Therefore, integrating renewable energy systems with improved power quality is essential to modern distribution systems.

Multifunctional renewable energy systems that can supply clean energy and offset power quality problems resulting from load side and PCC side have come under increased attention recently. In [4], the concept of a solar photovoltaic integrated distribution static compensator (PV-DSTATCOM) was presented. This system's twin functions include compensating for load current harmonics caused by nonlinear loads and producing power from renewable sources. In [5], a single-phase, multi-functional solar energy conversion system was suggested. This system was a single-phase distribution system that integrated active filtering and sustainable energy generating. In [6], a proposed variable DC-link voltage grid interfaced converter for three phase supply systems was made. This system offers an adjustable DC-link voltage in addition to active filtering and clean energy generation. Due to the DC-link voltage being modified in accordance with the voltage at the point of common coupling, load current efficiency is increased and its harmonic correction is satisfactory.

Recently, research has been conducted on the integration of distributed generation capability with universal active power filters, but the majority of the study on the integration of clean

International Journal on Recent and Innovation Trends in Computing and Communication
ISSN: 2321-8169 Volume: 11 Issue: 7
Article Received: *25 January 2023* ***Revised:*** *12 March 2023* ***Accepted:*** *30 June 2023*

energy systems with active filtering has focused on shunt compensated systems. In addition to PV integration, a unified power quality conditioner (UPQC), often referred to as a universal active power filter (UAPF), was proposed in [7], [8]. Because UAPF systems have both shunt and series active power filters, they improve both voltage and current quality. One drawback of the shunt active power filter is that it needs reactive power to control the PCC's voltage. Therefore, the shunt active filter is unable to meet both the need of voltage regulation and the requirement of preserving unity power factor (UPF) for grid current at the same time. In addition to injecting or drawing grid current at the UPF, the solar integrated universal active power filter (UAPF-PV) system controls load voltage.

The two primary purposes of the UAPF-PV are to mitigate problems with voltage and current quality and to supply power from PV arrays to the grid. Accurate and quick reference signal generation for the shunt and series active filter is essential to carrying out these tasks. In reference creation, one of the most important tasks is to extract the essential component of the distorted signal. P-q and d-q theory are two examples of reference frame conversion techniques that are frequently used algorithms for the control of active filters [3].Nevertheless, these methods necessitate several transformations, and when there is an imbalance in load, their dynamic performance declines. The least mean square technique (LMS) and the adaptive notch filter (ANF) are two examples of sophisticated methods for extracting fundamental components [9], [10]. Due to their intrinsic single-phase nature, these methods need two or more of these structures in addition to mathematical operations in order to extract the essential positive-sequence components. A damped SOGI approach has been developed in [11] for PV system reference signal generation. Using a damped SOGI filter, the fundamental active component of the load current in each phase of the system was retrieved using this technique. Based on sequence filters, complex filters, etc., another class of filters exists that are intrinsically three phase filters and are capable of directly extracting fundamental positive sequence components [12]. Additional sophisticated methods for obtaining the fundamental active component consist of approaches utilizing wavelet transforms and adaptive linear elements (ADA-LINE) [13-15]. Despite their excellent precision, there is a trade-off because of the increased computing load.

This work proposes a unique control technique for UAPF-PV control, based on second order sequence filter [12] based control for the shunt active filter and proportional resonant control for the series active filter [19]. The distorted load current's fundamental positive sequence component is estimated by the second-order sequence filter. To determine the amplitude of the basic active component of the load current, the fundamental positive sequence components are sampled at the right moment. After that, these are employed to produce reference signals that the shunt active filter uses to function. The active component of distorted load current may now be extracted with greater precision and high dynamic performance thanks to this technology. By adding the necessary voltage in series with the PCC voltage, the series active filter controls the load voltage during PCC voltage dips and rises. The main goals and benefits of this research are outlined below,

- Multifunctional topology that combines total power quality enhancement with renewable energy generation.
- Protects delicate loads from dips and rises in PCC voltage and adjusts for nonlinear current drawn by the load.
- By utilizing a single sample and hold operation in conjunction with a second order sequence filter and zero cross detection technique, the accuracy of extracting the load current active component of all three phases is improved.
- An assessment of the UAPF-PV system's dynamic and steady state performance under various scenarios, including changes in solar radiation intensity, imbalanced load removal, and dips and rises in PCC voltage.
- Utilizing a fuzzy logic controller (FLC) in place of traditional controllers such as PI or PID helps reduce the total harmonic distortion (THD) in grid current.

MATLAB/Simulink was used to validate the system response. The control algorithm is put into practice, producing the control signals required for the UAPFPV system. The system's steady state performance is examined to make sure it complies with IEEE-519 standards [18]. The system's dynamic performance is examined in scenarios including fluctuating solar irradiance, imbalanced nonlinear loads, and rises and falls in PCC voltages.

II. Configuration of PV-UAPF

Fig. 1 shows the UAPF-PV structure. The PV array is interfaced with the UAPF DC-bus through a boost DC-DC converter in a three phase, double stage topology. Filter inductors are used to connect the compensators to the distribution system. Through series transformers, the series active filter applies voltage in series with the PCC either in phase or in out of phase based on requirement of that particular condition.

In both series and shunt VSCs, ripple filters made of a series connection of resistors and capacitors are employed to filter out higher order harmonics produced by the switching action of series and shunt active filters.

The harmonical losses produced due to switching action of both VSC's in DC bus are estimated using any controller such as PI, PID and FLC. This is contributed into I_s^* as in form of I_{loss} component.

International Journal on Recent and Innovation Trends in Computing and Communication
ISSN: 2321-8169 Volume: 11 Issue: 7
Article Received: *25 January 2023* ***Revised:*** *12 March 2023* ***Accepted:*** *30 June 2023*

The double stage topology of VSC's DC bus voltage is regulated using a coupling capacitor. The proposed model is shown in Fig.1.

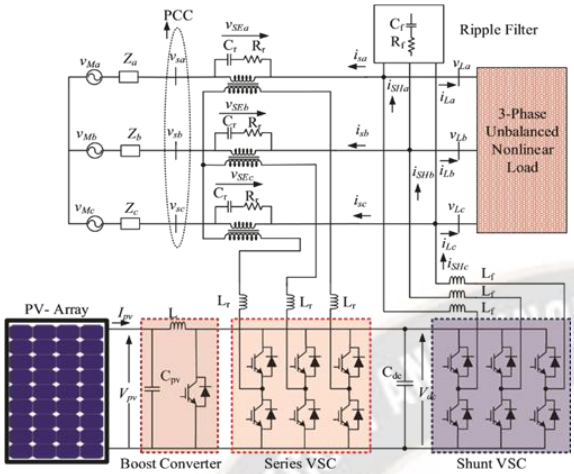

Fig. 1. System configuration of UAPF-PV

III. System Control

Protecting sensitive loads from PCC voltage dips and rises and compensating for harmonics caused by nonlinear loads are the main goals of UAPF-PV. UAPF-PV not only enhances power quality but also generates clean energy by feeding PV power into the distribution system. Here is a fuller explanation of the control features of both series and shunt active filters.

A. Control Configuration of Shunt Active Filter

Fig. 2(b) shows the block diagram for the shunt active filter's control. Using PI- Controller for Dc – Link control. Whereas, Fig. 2(c) shows control setup of same shunt active filter using FLC. The basic positive sequence component of the distorted load current is extracted in this control mechanism using a second order sequence filter. Fig. 2(a) depicts the second order sequence filter's structure. Since sequence filters capture the essential positive sequence components, they are naturally appropriate for three phase systems. The second order sequence filter's open-loop transfer function is provided as,

$$G_{sosf}(s) = \frac{K_1 K_2}{(s - j\omega' + K_2)(s - j\omega')} \quad (1)$$

The closed loop transfer function of 1 is given as,

$$Gcl_{sosf}(s) = \frac{K_1 K_2}{(s - j\omega' + K_2)(s - j\omega') + K_1 K_2} \quad (2)$$

In this structure, there are two controlling gains:K_1, K_2. A trade-off is made between the dynamic response and the precision of extracting the fundamental positive sequence component when determining the values of K_1 andK_2. A thorough examination of the filter gain selection is provided in [12]. The intended grid current is essentially represented by the shunt compensator reference signal. This indicates that the reference signal needs to have a power factor of unity and be balanced. Grid current due to fundamental active load power (I_{Lp}), grid current corresponding to PV power (I_{pvg}), and loss component corresponding to losses occurring due to switching action of semiconductor switches, losses in filters, etc. make up the magnitude of the grid current. The following equation provides this as,

$$I_s^* = I_{Lp} - I_{pvg} + I_{loss} \quad (3)$$

A second order sequence filter is used to determine the load current's fundamental frequency positive sequence component (FPSC). After estimating the FPSC of the load current, the magnitude of the load active current is retrieved by taking a sample of the current at the zero crossing of the load voltage's β component. The sampled value of the FPSC of the load current corresponds to the magnitude of the active component of the load current since the Clark transform of load voltages and load currents uses magnitude invariant transformation. Since the load is constant when the PCC voltage drops, more grid current must be used in order to maintain power balance. The following formula yields the comparable grid current for load active power:

$$I_{Lp} = K \times I_{Lap} \quad (4)$$

Where,

$$K = \frac{V_L^*}{V_s} \quad (5)$$

V_L^* is magnitude of reference load voltage V_s is the magnitude of PCC voltage.

The grid current magnitude corresponding to PV power is obtained by the following equation as,

$$I_{pvg} = \frac{2}{3}\frac{P_{pv}}{V_s} \quad (6)$$

where Vs is the PCC voltage magnitude and Ppv is the PV array power.

The Shunt Active Power Filter (SAPF) is designed to eliminate unwanted harmonics caused by non-linear loads such as multiple Compact Fluorescent Lamps (CFLs) and to improve the overall power factor in 3-phase 4-wire systems. This technology is crucial in maintaining power quality and ensuring efficient operation of electrical systems by compensating for reactive power and harmonics.

The DC-bus voltage of the UAPF-PV can be controlled at a desired value by any conventional controllers like proportional integral (PI) controller or by any more accurate controllers like Fuzzy Logic Controller (FLC). The component that

International Journal on Recent and Innovation Trends in Computing and Communication
ISSN: 2321-8169 Volume: 11 Issue: 7
Article Received: *25 January 2023* ***Revised:*** *12 March 2023* ***Accepted:*** *30 June 2023*

corresponds to losses in the filter and converter circuits is provided by the controller.

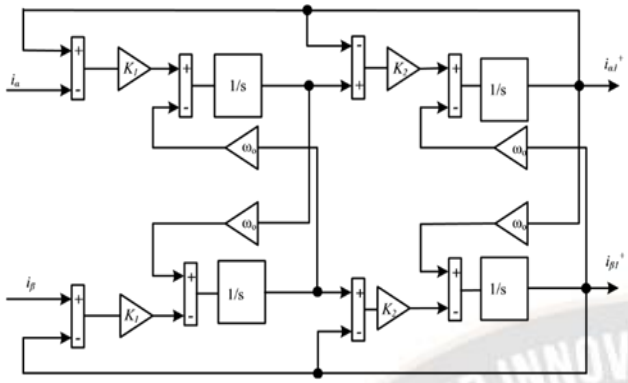

(a) Structure of second order sequence filter.

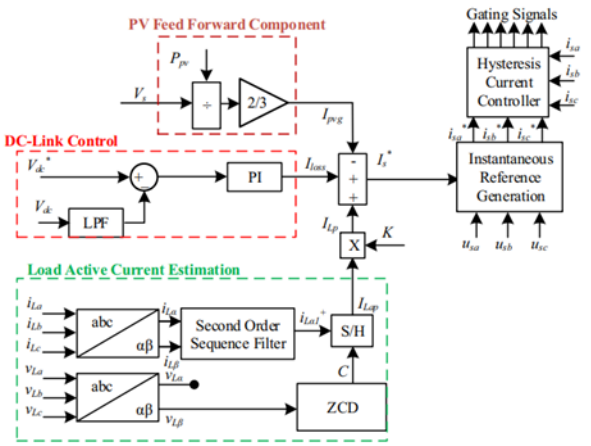

(b) Shunt Compensator Control Structure with PI Controller

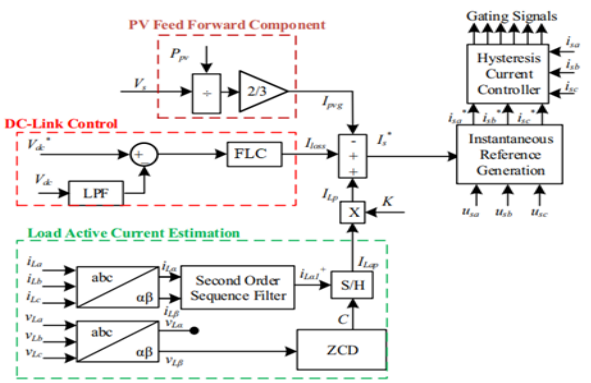

(c) Shunt Compensator Control Structure with FLC

Fig. 2. Shunt Compensator Control Based on second order sequence filter.

The DC-link PI controller's control equation is provided as:

$$I_{loss}(n) = I_{loss}(n-1) + K_p(\Delta e_{vdc} + K_i e_{vdc}(n)) \quad (7)$$

where I_{loss} is the output of PI controller which is also the loss component of UAPF-PV, K_p and K_i are the gains of PI controller.

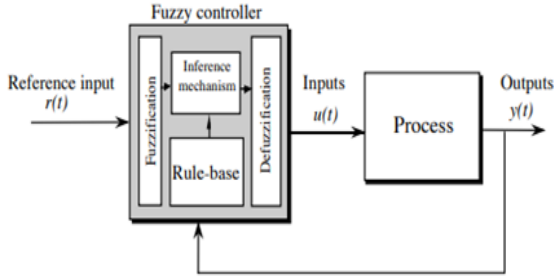

Fig.3 Fuzzy controller

From Fig.3.The DC-link FLC's control equation is provided as:

$$I_{loss}(n) = I_{loss}(n-1) + \Delta e_{vdc} \rightarrow FLC_{(i/o)_1} + e_{vdc}(n) \rightarrow FLC(i/o)_2 \quad (8)$$

where I_{loss} is the output of FLC which is also the loss component of UAPF-PV, Δe_{vdc} is the difference in DC-link voltage error between the present and past sampling time which 2nd input to FLC. e_{vdc} is the DC-link voltage error which is the 1st input to FLC.

The following formulas are used to derive the PCC voltage in-phase templates and the magnitude of PCC voltage V_s:

$$V_s = \sqrt{\frac{2}{3}(V_{sa}^2 + V_s b^2 + V_s c^2)} \quad (9)$$

$$u_{sa} = \frac{v_{sa}}{V_s}, u_{sb} = \frac{v_{sb}}{V_s}, u_{sc} = \frac{v_{sc}}{V_s} \quad (10)$$

To create instantaneous shunt active filter reference currents ($i_{sa}^*, i_{sb}^*, i_{sc}^*$), the reference magnitude is multiplied by templates of PCC voltages.

$$i_{sa}^* = I_s^* \times u_{sa}, i_{sb}^* = I_s^* \times u_{sb}, i_{sc}^* = I_{sc}^* \times u_{sc} \quad (11)$$

The error between ($i_{sa}^*, i_{sb}^*, i_{sc}^*$) and ($i_{sa}, i_{sb}, i_{sc}$) is passed through hysteresis controller which generates gating pulses for controlling the shunt compensator.

B. Control Configuration of Series Active Filters

Fig.4 displays the system's control arrangement. In the − β domain, the control of a series active filter is implemented. The PCC and load voltages have the same phase thanks to control over the series active filter. The voltages of the instantaneous reference load are produced as,

$$v_{La}^* = V_L \times u_{sa} \quad (12)$$

$$v_{Lb}^* = V_L \times u_{sb} \quad (13)$$

$$v_{Lc}^* = V_L \times u_{sc} \quad (14)$$

International Journal on Recent and Innovation Trends in Computing and Communication
ISSN: 2321-8169 Volume: 11 Issue: 7
Article Received: *25 January 2023* ***Revised:*** *12 March 2023* ***Accepted:*** *30 June 2023*

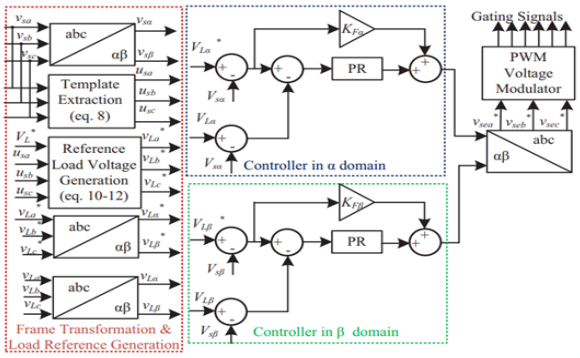

Fig.4. Series Active Filter Control Structure

Then, the α − β domain is obtained from these reference load voltages. Two sets of damped proportional controllers are implemented for the α and β components, in addition to a feedforward circuit, to control the series active filter. The reference series active filter voltage ($v^*_{se\alpha}$) in the α domain can be found as,

$$v^*_{se\alpha} = v^*_{L\alpha} - v_{s\alpha} \quad (15)$$

The series active filter voltage ($v_{se\alpha}$) is obtained as,

$$v_{se\alpha} = v_{L\alpha} - v_{s\alpha} \quad (16)$$

Damped proportional resonant controller is provided the error between $v^*_{se\alpha}$ and $v_{se\alpha}$. Damped proportional resonant (PR) controllers have the benefit of having very high gain for the intended frequency and adjustable gain depending on the cut-off frequency. The feedforward path's output and the PR controller's output are combined. The feedforward path provides the majority of the control signal, and the PR controller accommodates for filter circuit dropouts that are not taken into consideration when calculating references. In the same way, the β domain implements the control function. After obtaining control signals in the α − β domain, the signals are transformed back into stationary frames and sent to a PWM modulator, which produces gating pulses for the series active filter.

C. Setting-up Fuzzy Logic Controller

A block diagram of a fuzzy control system is shown in Fig 3. The fuzzy controller is composed of the following four elements:

1. A *rule-base* (a set of If-Then rules), which contains a fuzzy logic quantification of the expert's linguistic description of how to achieve good control and the standard Fuzzy Rules for 7 membership functions are used for current study which are depicted in Table I.
2. An *inference mechanism* (also called an "inference engine" or "fuzzy inference" module), which emulates the expert's decision making in interpreting and applying knowledge about how best to control the plant.
3. A *fuzzification interface*, which converts controller inputs into information that the inference mechanism can easily use to activate and apply rules.
4. A *defuzzification interface*, which converts the conclusions of the inference mechanism into actual inputs for the process.

Selecting the controller's inputs and outputs, or inputs to the plant, can be more challenging. Essentially, if the right control inputs are available then, it can guide the system in the directions required to achieve high performance operation. For the controller inputs and output which are depicted in Fig. 5 are taken as:

Input 1: The error signal estimated from the difference of V_{DC}^* i.e., Dc reference voltage and instantaneous value of V_{DC}.

Input 2: The change in Error signal (Input 1) from the previous value to present value.

Output: Loss component (I_{Loss}) estimated after applying rules from Table I on inputs 1, 2.

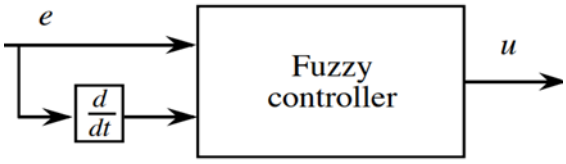

Fig.5. Fuzzy Controller's inputs and output

Table I. Mamdani Rule Based Model

Output		**Change in Error (*input2*)**						
		NB	**NM**	**NS**	**ZE**	**PS**	**PM**	**PB**
Error	**NB**	NB	NB	NB	NB	NM	NS	ZE
	NM	NB	NB	NB	NM	NS	ZE	PS
	NS	NB	NB	NM	NS	ZE	PS	PM

International Journal on Recent and Innovation Trends in Computing and Communication
ISSN: 2321-8169 Volume: 11 Issue: 7
Article Received: *25 January 2023* ***Revised:*** *12 March 2023* ***Accepted:*** *30 June 2023*

(*input1*)	**ZE**	NB	NM	NS	ZE	PS	PM	PB
	PS	NM	NS	ZE	PS	PM	PB	PB
	PM	NS	ZE	PS	PM	PB	PB	PB
	PB	ZE	PS	PM	PB	PB	PB	PB

defuzzifier is generally required only when the Mamdani Fuzzy Model is used for designing a controller. There are other types of architectures that can be used are: Tagaki-Sugeno Fuzzy Model, Tsukamoto Fuzzy Model. Mamdani model is preferred here because it follows the Compositional Rule of Inference strictly in its fuzzy reasoning mechanism.

The Centroid of Area (COA) is one of the most popular techniques used for defuzzification, as it is reminiscent of the calculation of expected values of probability distributions. It can be defined as follows:

$$Z_{COA} = \frac{\int_z \mu_A(z) z \, dz}{\int_z \mu_A dz} \qquad (17)$$

Where $\mu_A(z)$ is the aggregated output MF.

D. Control of Boost DC-DC Converter

The PV array is operated at its maximum power point by the boost DC-DC converter. For this, the boost converter is controlled via an MPPT algorithm. The MPPT algorithms that are frequently employed are the fractional open circuit voltage, incremental conductance (INC) approach, and perturb and observe (P&O) technique [17-18]. In this work, the PV array's maximum power operating point is tracked using P&O approach. The algorithm determines the proper duty ratio for regulating the boost converter by detecting the power and voltage levels of the PV array both in the past and present. The duty ratio for the subsequent cycle in the P&O approach is obtained as follows.

$$d_{boost}(n+1) = d_{boost}(n) + D_{step}.sgn(\Delta P_{pv}) \qquad (18)$$

where $d_{boost}(n+1)$ is the duty ratio for next MPPT sampling interval of boost converter, $d_{boost}(n)$ is the duty ratio in the current MPPT sampling interval, D_{step} is the duty ratio step size and ΔP_{pv} is the difference in PV array power between the current sampling interval and past sampling interval.

IV. Experimental Evaluation

The performance of second order sequence filter based UAPF-PV is validated on Simulink in the MATLAB. Table II gives the parameters used in simulation.

Firstly, PI controller was used for the DC Link voltage control, during which the steady state for the output (I_{loss}) was obtained in an abrupt manner it caused overall THD of grid current to be in range of 2% to 5% which is according to IEEE - 519 as well under all dynamic conditions[18]. Now, a more accurate FLC controller is used for the DC link voltage control instead of the traditional PI controller, during which the steady state for the output (I_{loss}) was obtained in a more gradual and smooth manner it caused overall THD of grid current to be significantly lower than it was with the PI controller which is illustrated in Table III under all dynamic conditions.

Table II. Experimental parameters

Parameter	**Values**
PCC voltage	v_s = 220 V, f = 50 Hz
Nonlinear Load	Rectifier with R-L: 1.12 kW
DC-bus Voltage	V_{dc} = 380 V
DC-bus Capacitor	C_{dc} = 3.3 mF
Boost Inductor	L = 4mH
PV array Capacitor	C_{pv} = 100μF
Shunt Active Filter Inductor	L_s = 4 mH
Series Active Filter Inductor	L_{se} = 0.5 mH
Sampling Time	T_s = 33.33 μs
DC-bus PI controller	K_p = 0.2, K_i = 0.15
DC-bus Fuzzy Logic controller	*Inputs 1,2 – range = [-1 1]* *NB = [-1.667 -1 -0.8]*

International Journal on Recent and Innovation Trends in Computing and Communication
ISSN: 2321-8169 Volume: 11 Issue: 7
Article Received: *25 January 2023* ***Revised:*** *12 March 2023* ***Accepted:*** *30 June 2023*

	NM = [-1 -0.8 0] *NS = [-0.8 -0.4 0]* *ZE = [-0.01 0 0.01]* *PS = [0 0.4 0.8]* *PM = [0 0.8 1]* *PB = [0.8 1 1.1]* *Output – range = [-1 1]* *NB = [-1.1 -1 -0.8]* *NM = [-1 -0.8 -0.425]* *NS = [-0.8 -0.425 0]* *ZE = [-0.425 0 0.425]* *PS = [0 0.425 0.8]* *PM = [0.425 0.8 1]* *PB = [0.8 1 1.1]*
Second Order Sequence Filter Gains	$K1$=100,$K2$=250
Series Active Filter PR controller	$KP\alpha-\beta$ = 1;
$KR-\alpha-\beta$ = 600, KFF = 1 LPF cut off frequency	f_{LPF} = 10 Hz
PV Array	P = 4.0 kW, V_{oc} = 350 V, I_{sc} = 14 A V_{mpp} = 301 V, I_{mpp} = 13.272 A

Clearly, many choices for the shape of the membership function are possible (e.g., triangular, trapezoidal shapes and Gaussian membership functions), and these will each provide a different meaning for the linguistic values that they quantify. For this we choose triangular membership function and see Tables II for a mathematical characterization.

A. UAPF-PV Response under Steady State Conditions with Fuzzy Logic Controller

The UAPF-PV Responses under Steady State Conditions with PI – controller was well illustrated in [1]. Now, the UAPF-PV Responses under Steady State Conditions with FLC are,

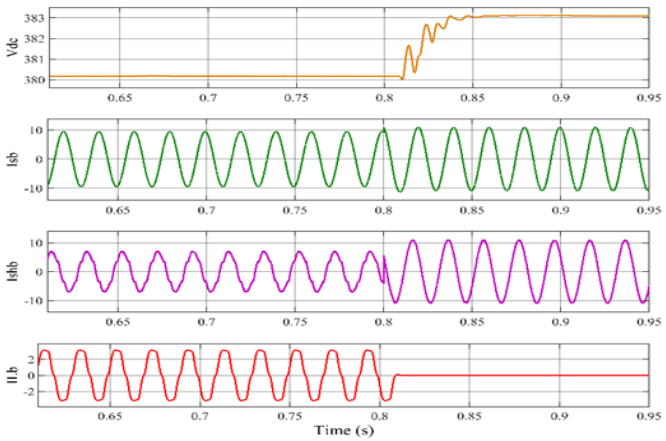

(a) Performance under Load Removal

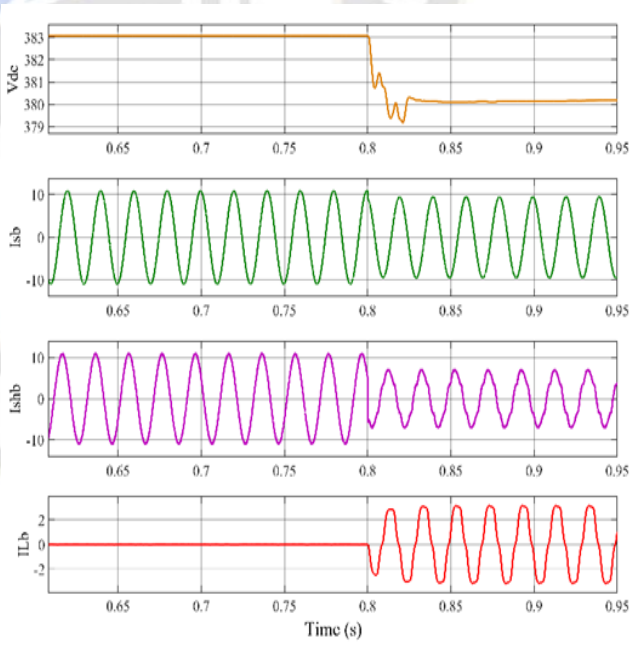

(b) Performance under Load Addition

Fig.6. Dynamic Performance under load Unbalance Condition

Fig.6. presents the system performance under load disturbance conditions. In this test, the load in phase 'b' of the system is entirely removed or included, and its impact on the grid current

International Journal on Recent and Innovation Trends in Computing and Communication
ISSN: 2321-8169 Volume: 11 Issue: 7
Article Received: *25 January 2023* ***Revised:*** *12 March 2023* ***Accepted:*** *30 June 2023*

on the same phase is observed. Fig 6(a) and 6(b) show the performance of UAPF-PV under phases of load removal and load addition, respectively.

The signals captured are V_{dc}, i_{sb}, i_{shb} and i_{Lb}. All the currents signals are of phase 'b'. Even with an unbalanced and nonlinear load current, the UAPF-PV shunt active filter keeps the grid current sinusoidal. The voltage of the DC-link is controlled. I_{sb} rises as a result of a decrease in load.

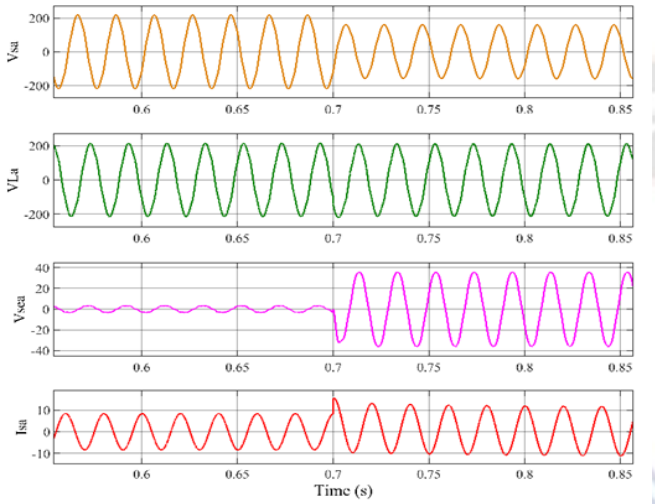

(a) Performance under PCC Voltage Dip Condition

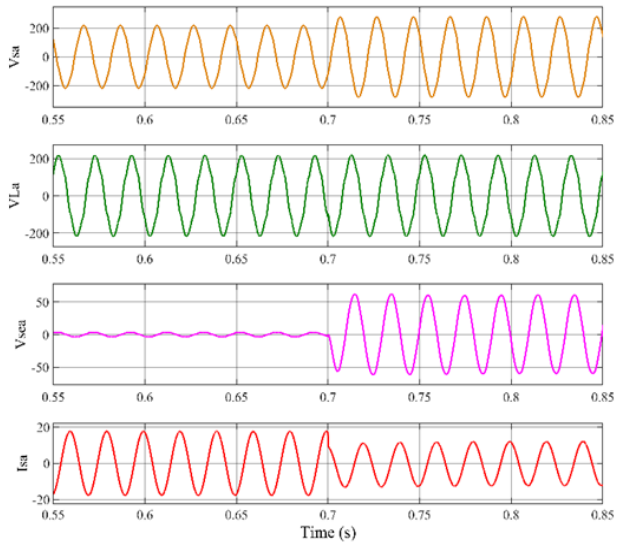

(b) Performance under PCC Voltage Swell Condition

Fig.7. Dynamic Performance under PCC Voltage dip/rise Condition

Fig. 7 present the performance under nominal, dip and rise in PCC voltages. Though the PCC voltage undergoes dip from nominal value to 160 V and increases to 275 V during voltage rise condition, the PCC load voltages are maintained within 1% of the desired regulation value of 220 V. It is to be noted that while the load current is nonlinear with total harmonic distortion (THD) of approximately 23%. The grid current has been maintained under 1% under all conditions.

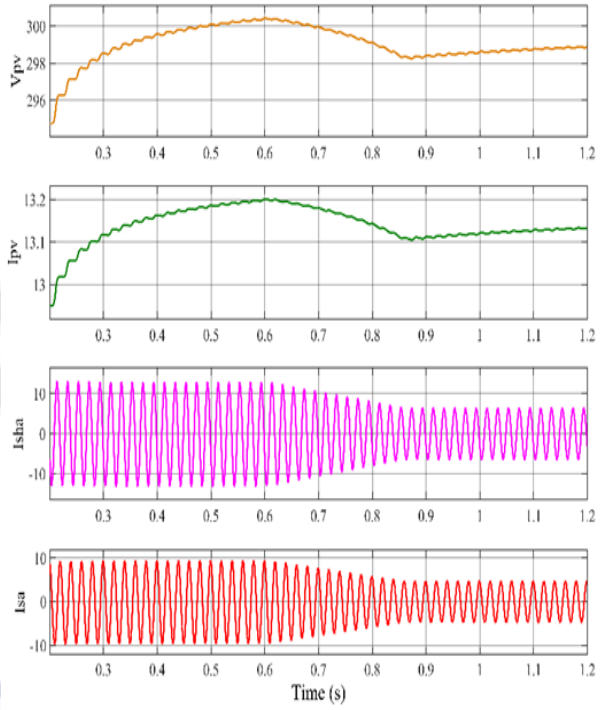

Fig. 8. UAPF-PV Response under irradiation Change Condition

The signals captured in Fig.7 are $v_{sab}, v_{Lab}, v_{seab}, and\ i_{sa}$. The PCC voltage reduces to 0.75pu while during swell the PCC voltage rises to 1.25pu. The series active filter injects appropriate voltage to maintain load voltage at desired value of 220 V. Fig. 8 shows the system's behaviour as sun irradiation varies. Under these circumstances where solar radiation intensity is dropping from 1000 W/m^2 to 500 W/m^2, the system's performance is recorded. It is evident that in each of these scenarios, the DC-link voltage remains constant.

B. Control Signals for UAPF-PV

Grid current corresponding to load active current (KI_{La}), loss component (I_{loss}), grid current corresponding to injected PV array power (I_{pvg}), and magnitude reference grid current (I_s^*) are shown in fig.9, which serves as a reference for the shunt active filter, are the signals that were collected. Based on 3, the reference current (I_s^*) is determined. After phase "b" load has been removed, the signals are captured. The load current is shown to be decreasing. As result, I_s^* rises, as shown by Equation (3).

The essential internal signals that regulate the shunt and series active filters are shown in Fig. 10. The salient internal signals for the shunt active filter's reference current production are shown in Fig.10(a).

International Journal on Recent and Innovation Trends in Computing and Communication
ISSN: 2321-8169 Volume: 11 Issue: 7
Article Received: *25 January 2023* ***Revised:*** *12 March 2023* ***Accepted:*** *30 June 2023*

The salient internal signals that regulate the series active filter are shown in Fig. 10(a). The signals are captured when the load has been removed from the 'b' phase the moment when load gets detached, reference signals are produced .The UAPF-PV control signals are shown in Fig10. The salient signals in the second order sequence filter are shown in Fig. 10(b). Phase "b" load current, $i_{L\alpha}, i_{L\beta}$, and the α component of the fundamental positive sequence component $i^{+}_{L\alpha 1}$ are the signals that were recorded. It can be observed that the second order sequence filter extracts the FPSC of the load current within a cycle upon instantaneous removal of the load in phase "b."

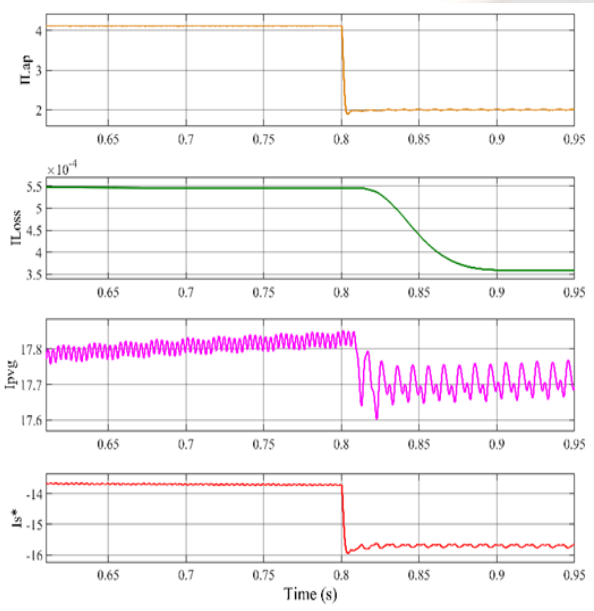

Fig.9. Salient Signals of grid current reference generation

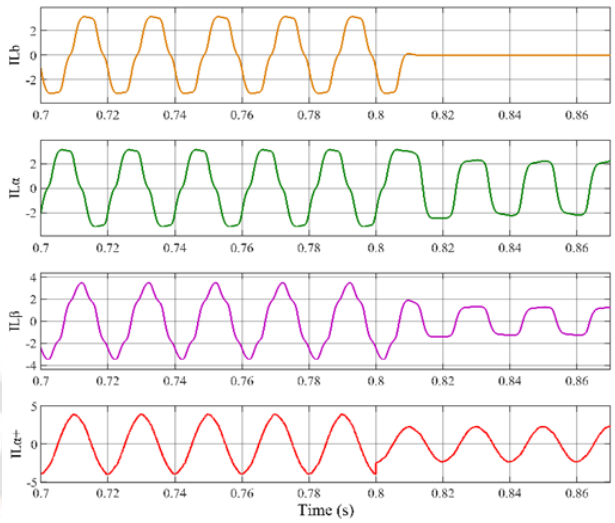

(a) Salient Signals in Shunt Active Filter Control

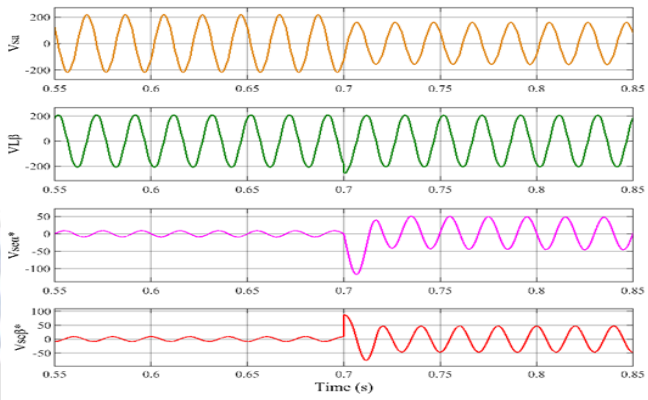

(b) Salient Signals in series active filter Control

Fig. 10. Salient Signals in UAPF-PV Control

Table III. Comparison of PI And FLC Controllers In Thd Reduction

parameter	**Controller**	**Case1: Load removal**	**Case2: Load Addition**	**Case3: Under Voltage Dip**	**Case4: Under Voltage Swell**	**Case5: under irradiation Change Condition**
I_{sabc}	**PI**	2.62%	2.59%	4.91%	4.32%	3.68%
I_{Labc}		21.46%	21.47%	21.65%	21.77%	21.47%
I_{sabc}	**FLC**	0.69%	0.58%	3.91%	3.12%	2.24%
I_{Labc}		8.59%	6.33%	8.23%	7.96%	6.32%

From the Table. III it can be observed that the Fuzzy Controller has potentially reduced the THD in grid current as well as in Load current as compared to traditional PI- Controller.The graphical representation of this comparison under dynamic load imbalance, PCC voltage dip/rise and irradiance variation is shown in Fig. 11.

International Journal on Recent and Innovation Trends in Computing and Communication
ISSN: 2321-8169 Volume: 11 Issue: 7
Article Received: *25 January 2023* ***Revised:*** *12 March 2023* ***Accepted:*** *30 June 2023*

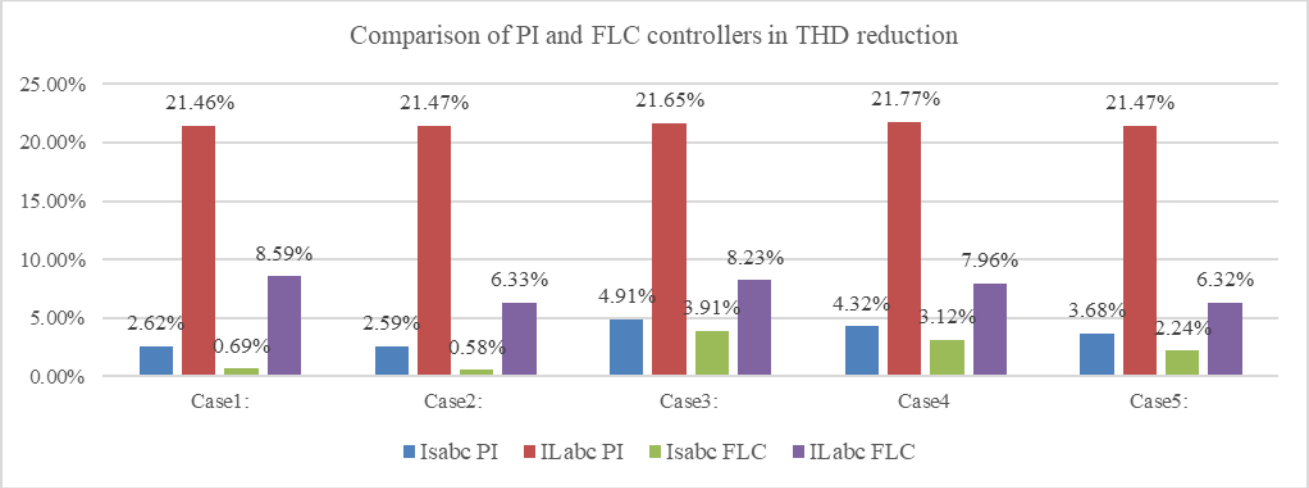

Fig.11. Chart representation of PI & FLC under all conditions

Study Limitations

The study was conducted in a simulated environment (MATLAB/Simulink), which might not fully indicate real-world conditions. The performance of the proposed system under actual environmental and operational conditions, such as variable weather and fluctuating loads, needs to be validated through real-world testing. The study focused mainly on comparing PI and Fuzzy Logic Controllers (FLC) for DC link voltage control. Other advanced control strategies, such as Model Predictive Control (MPC) and Sliding Mode Control (SMC), were not explored which limits the actual comparison and optimization. The study demonstrated the improved Total Harmonic Distortion (THD) reduction with FLC, but it did not include the long- term performance and degradation effects of the system components under continuous operation.

The economic feasibility and cost-benefit analysis of implementing these advanced control methods in large-scale PV systems were not addressed. While the study mentioned the integration of energy storage solutions and hybrid systems as a future scope the impact of incorporating batteries, supercapacitors, and hybrid renewable energy sources on system performance and stability requires further examination. Real-time implementation can reveal challenges such as latency, computational burden, and integration issues that were not apparent in the simulation environment. Although the study assessed system performance under various dynamic conditions like load fluctuations and PCC voltage dips/rises, a more extensive range of scenarios, including extreme weather conditions and grid disturbances, should be evaluated to ensure robustness and reliability.

Conclusion

An evaluation has been conducted on the performance of a new fuzzy control method for solar PV systems with universal active filtering. Using a zero cross detection method in conjunction with a fuzzy-based second order sequence filter, the essential positive sequence component of nonlinear load current is retrieved. A feed forward component and a proportional resonant controller constructed in the − domain are used to regulate the series active filter.

When there are disturbances like variations in solar radiation, load fluctuations, and PCC voltage dips and rises, the system functions satisfactorily. In addition to enhancing power quality, the technology feeds grid power from photovoltaic arrays. When compared to traditional PI control methods, the system performs better with the suggested fuzzy control having a marginally lower computing load.

Future Scope

The future scope of this project involves exploring and implementing advanced methodologies to further enhance the performance and efficiency of solar photovoltaic systems. Main advancements include utilizing more advanced Maximum Power Point Tracking (MPPT) techniques, such as ANFIS and neural networks, which can offer improved adaptability and accuracy under varying environmental conditions. Combining traditional controllers with advanced methods like model predictive control or sliding mode control, can optimize the regulation of DC link voltage and improve overall system robustness. The integration of PV systems with other renewable energy sources, such as wind or hydro power, can create hybrid systems that provide more consistent and reliable energy output. Implementing microgrids that combine PV systems with other renewable sources and energy storage like battery system can offer localized and robust power solutions. Further research could explore the integration of energy storage solutions and the development of smart grid technologies to enhance the reliability and stability of power supply.

References

[1] B. Singh and S. Devassy "Implementation of Solar Photovoltaic System with Universal Active Filtering Capability," *IEEE Trans. Ind. Appl.*, vol. 55, Issue: 4, July-Aug. 2019.

[2] S. J. Pinto, G. Panda, and R. Peesapati, "An implementation of hybrid control strategy for distributed generation system interface using xilinx system generator," *IEEE Transactions on Industrial Informatics*, vol. 13, no. 5, pp. 2735–2745, Oct 2017.

[3] B. Singh, A. Chandra, K. A. Haddad, *Power Quality: Problems and Mitigation Techniques*. London: Wiley, 2015.

[4] B. Singh, M. Kandpal, and I. Hussain, "Control of grid tied smart pv-dstatcom system using an adaptive technique*," IEEE Transactions on Smart Grid*, vol. PP, no. 99, pp. 1–1, 2017.

[5] Y. Singh, I. Hussain, S. Mishra, and B. Singh, "Adaptive neuron detection-based control of single-phase spv grid integrated system with active filtering," *IET Power Electronics*, vol. 10, no. 6, pp. 657–666, 2016.

[6] C. Jain and B. Singh, "An adjustable dc link voltage-based control of multifunctional grid interfaced solar pv system," *IEEE Journal of Emerging and Selected Topics in Power Electronics*, vol. 5, no. 2, pp. 651–660, June 2017.

[7] S. Devassy and B. Singh, "Modified pq-theory-based control of solar-pv-integrated upqc-s*," IEEE Trans. Ind. Appl.*, vol. 53, no. 5, pp. 5031– 5040, Sept 2017.

[8] S. Devassy and B. Singh, "Design and performance analysis of three phase solar pv integrated upqc," *IEEE Transactions on Industry Applications*, vol. PP, no. 99, pp. 1–1, 2017.

[9] R. Chilipi, N. A. sayari, K. H. A. Hosani, and A. R. Beig, "Adaptive notch filter based multipurpose control scheme for grid-interfaced three-phase four-wire dg inverter," *IEEE Trans. Ind. Appl.*, vol. PP, no. 99, pp. 1–1, 2017.

[10] M. Badoni, A. Singh, and B. Singh, "Comparative performance of wiener filter and adaptive least mean square-based control for power quality improvement," *IEEE Trans. Ind. Electron.*, vol. 63, no. 5, pp. 3028–3037, May 2016.

[11] B. Singh, S. Kumar, and C. Jain, "Damped-SOGI based control algorithm for solar pv power generating system," *IEEE Trans. Ind. Appl.*, vol. 53, no. 3, pp. 1780–1788, May 2017.

[12] Z. Xin, R. Zhao, P. Mattavelli, P. C. Loh, and F. Blaabjerg, "Reinvestigation of generalized integrator-based filters from a first-order-system perspective," *IEEE Access*, vol. 4, pp. 7131–7144, 2016.

[13] M. Qasim and V. Khadkikar, "Adaline based control strategy for threephase three-wire upqc system," in 2014 16th International Conference on Harmonics and Quality of Power (ICHQP), May 2014, pp. 586–590.

[14] N. Karthikeyan, M. K. Mishra, and B. K. Kumar, "Complex wavelet-based control strategy for upqc," in *2010 Joint International Conference on Power Electronics, Drives and Energy Systems 2010 Power India*, Dec 2010, pp. 1–6.

[15] A. B. Shitole, H. M. Suryawanshi, G. G. Talapur, S. Sathyan, M. S. Ballal, V. B. Borghate, M. R. Ramteke, and M. A. Chaudhari, "Grid interfaced distributed generation system with modified current control loop using adaptive synchronization technique," *IEEE Trans. Ind. Electron.*, vol. 13, no. 5, pp. 2634–2644, Oct 2017.

[16] N. Kumar, I. Hussain, B. Singh, and B. K. Panigrahi, "Framework of maximum power extraction from solar pv panel using self-predictive perturb and observe algorithm," *IEEE Transactions on Sustainable Energy*, vol. PP, no. 99, pp. 1–1, 2017

[17] S. Hota, M. K. Sahu, and J. M. R. Malla, "A Standalone PV System with a Hybrid P&O MPPT Optimization Technique", Eng. Technol. Appl. Sci. Res., vol. 7, no. 6, pp. 2109–2112, Dec. 2017.

[18] https://doi.org/10.48084/etasr.3889

[19] J. C. Das, "Harmonic Distortion Limits According to Standards," in Power System Harmonics and Passive Filter Designs , IEEE, 2015, pp.427-451, doi: 10.1002/9781118887059.ch10. keywords: {Harmonic analysis;Power harmonic filters;Harmonic distortion;IEC Standards},

[20] T. Demirdelen, R. I. Kayaalp, and M. Tumay, "Modeling and Analysis of a Multilevel Parallel Hybrid Active Power Filter", Eng. Technol. Appl. Sci. Res., vol. 6, no. 3, pp. 976–981, Jun. 2016. https://doi.org/10.48084/etasr.665.

Authors Profile

Mr.D VenkataBrahmanaidu was born in Andhra- Pradesh, India. He received his B. Tech degree in Electrical and Electronics Engineering from JNTU Hyderabad, Telangana, India in 2010. He received his M. Tech degree in Power Electronics and Electrical Drives from JNTU Hyderabad, Telangana in 2014. He is currently pursuing Ph. D in Electrical- Engg, Annamalai University and working as Assistant Professor in at Narayana Engineering College, Nellore, Andhra Pradesh from, India. His areas of interests are

Microgrid, Renewable Energy Sources Power Electronics, Electrical drives and the application of Soft Computing techniques. He has published his works in various international and national journals. Having Life Memberships of ISCA, IE(India), ISTE, IAENG and IFERP.

Dr. R. Thamizhselvan serves as an Associate Professor of Electrical Engineering at Annamalai University, located in Tamil Nadu, India. He earned his Bachelor's degree in Electrical and Electronics Engineering from Annamalai University in 2004, followed by a Master of Engineering in Power Systems in 2008, also from Annamalai University. He furthered his academic pursuits by completing his Ph.D. in Electrical Engineering in 2017.Currently, he is on assignment at Government Technical Institutions under the Directorate of Technical Education in Chennai. His research focuses including Power System Security, Renewable Energy, Microgrid, and the application of Soft Computing techniques in Power Systems. He is a lifetime member of IOE(India), ISTE&IAENG.

Dr. Ch. Chengaiah, Professor in Sri Venkateswara University, Tirupati, Andhra Pradesh He received his B. Tech degree in Electrical and Electronics Engineering from S.V.U College of Engineering, Tirupati, AP in 1999. He received his M.E degree in Power Systems from National Institute of Technology formerly called as REC, Tiruchirapalli, TN in 2000 and He received his Ph.D. degree in Power Systems Operation and Control from Sri Venkateswara University in 2013. With 21 years of teaching experience under his girdle, he has successfully concluded three funded research projects. His research interests include Power System and Control Engineering, Renewable Energy Systems, Power Electronics and Drives.